

Revised Abstract for
End-Stage Transition Workshop
15-18 August 1993
Hairpin Vortices and the Final Stages of Transition

Abstract

A spatially developing direct numerical simulation has been performed for flow over a flat plate that is subjected to a one-time fluid injection through an elongated slit in the wall. The flow parameters have been chosen to closely approximate the experimental conditions of Haidari, Taylor, and Smith (AIAA-89-0964). A hairpin vortex quickly develops near the upstream end of the slit, and a pair of necklace vortices form around the slow-moving injected fluid. As seen in the experiments and reported in Haidari and Smith (in review, *JFM*), the hairpin vortex spawns both in-line and sidelobe secondary vortices. However, no subsidiary vortices (those formed by the inviscid deformation of a vortex-line bundle) are observed. At later times, a set of three different types of vortices are identified: hairpin vortex structures with heads that rise away from the wall, horseshoe-shaped vortices that do not rise out of the boundary layer, and quasi-streamwise vortices. These structures interact with each other and with the wall layer to generate new vortices that are similar in structure to those mentioned above, although a particular parent vortex may have an offspring that more nearly resembles another member of the set. Perturbation velocity and vertical vorticity contours reveal an arrowhead shape of the highly disturbed region that is reminiscent of a turbulent spot. Spatially averaged velocity profiles in the highly disturbed area are nonlaminar, but as yet do not show typical law-of-the-wall behavior.

Bart Singer

Fax: (804) 864-6134

E-mail: b.a.singer@larc.nasa.gov

HAIRPIN VORTICES
and the
FINAL STAGES OF TRANSITION

Bart A. Singer

Acknowledgments
Ron Joslin,
Surya Dinavahi, Craig Streett,
Mary Adams

NUMERICS

- **Main Points**
 - **Spatially developing direct numerical simulation**
 - **Buffer domain technique used for outflow conditions**
 - **Stretched vertical and streamwise grid**
- **Other Details**
 - Compact differences for velocity in streamwise direction
 - Chebyshev series expansion in wall-normal direction
 - * Gauss-Lobatto pts. for u , v , w and 2D p
 - * Gauss pts. for 3D p component
 - Fourier cosine/sine series in spanwise direction
 - Fractional time-step splitting
 - * Crank-Nicolson implicit for normal diffusion terms
 - * Runge-Kutta explicit for all other terms
 - * Influence-matrix technique for the 2D pressure component
 - * Direct solves for the 3D pressure component

SUMMARY

- **What's Old?**
 - Injection produces hairpin vortex
 - Additional vortex heads appear where legs converge
 - Necklace vortex develops around injected flow
 - Flow becomes increasingly complex
 - Disturbed region takes on arrowhead shape like turbulent spot

- **What's New?**
 - Regenerative processes
 - * New hairpin vortices appear
 - * Subsidiary horseshoe vortices form under other vortices
 - * Quasi-streamwise vortices form under other vortices
 - Turbulent spot development length is long
 - * Highly intermittent (large velocity gradients) from start
 - * Fully turbulent characteristics require more distance

Figure 1: Schematic of computational domain and injection slot. The solid black region along the symmetry line shows the location of the injection slot. The schematic in (b) shows the vertical velocity distribution along the symmetry line during times of maximum injection ($0.5 \leq t \leq 4.5$). The view on the lower left illustrates the spanwise distribution of vertical velocity. The Reynolds numbers are based on the local displacement thickness. Lengths are nondimensionalized on the displacement thickness at $Re_{\delta^*} = 530$.

Figure 2: Side view of isopressure surfaces at $t = 15.0$. Total velocity vectors on the centerline upstream of the injection slot are illustrated on the left. The thin black horizontal line represents the region over which fluid injection occurred. A streamline starting just upstream of the injection region spirals around a streamwise elongated low pressure region.

Figure 3: Looking downstream at primary and secondary high-pressure regions at $t = 21.75$. Cross-stream velocity vectors at $x = 55.4$.

Figure 4: Streamwise velocity profile at $x = 65.2$, $t = 15.0$. The Blasius profile at the same location is included for comparison.

Figure 5: Side view of high- and low-pressure regions ($p = \pm 0.035$) at $t = 35.70$. The low-pressure region resembles a hairpin vortex. The Blasius velocity profile is shown on the left. The downstream end of the hairpin vortex is at $x = 65.7$; the velocity profile is at $x = 56.9$.

Figure 6: Side view of high- and low-pressure regions ($p = \pm 0.035$) at $t = 50.25$. The Blasius velocity profile is shown on the left. The low-pressure zones show the primary hairpin vortex, a secondary vortex head, and a subsidiary vortex forming underneath each vortex leg. The downstream end of the hairpin vortex is at $x = 76.5$; the velocity profile is at $x = 64.3$.

Figure 7: Downstream view of low-pressure regions ($p = -0.035$) at $t = 50.25$. The surfaces are somewhat transparent so that perturbation velocity vectors at $x = 71.8$ can be seen.

Figure 8: Downstream view of high- and low-pressure regions ($p = \pm 0.035$) at $t = 50.25$. Perturbation velocity vectors at $x = 67.3$ are shown.

Figure 9: Plan view of high- ($p = 0.03$) and low-pressure ($p = -0.035$) regions at $t = 80.70$. The downstream edge of the vortex head is at $x = 94.0$. The upstream end of the high-pressure region is at $x = 80.5$.

Figure 10: Plan view of high- ($p = 0.02$) and low-pressure ($p = -0.035$) regions at $t = 97.20$. The downstream edge of the vortex head is at $x = 103.6$. The upstream end of the high-pressure region is at $x = 88.6$.

Figure 11: Side view of high- ($p = 0.02$) and low-pressure ($p = -0.035$) regions at $t = 97.20$. The Blasius profile is shown at the left at $x = 86.9$.

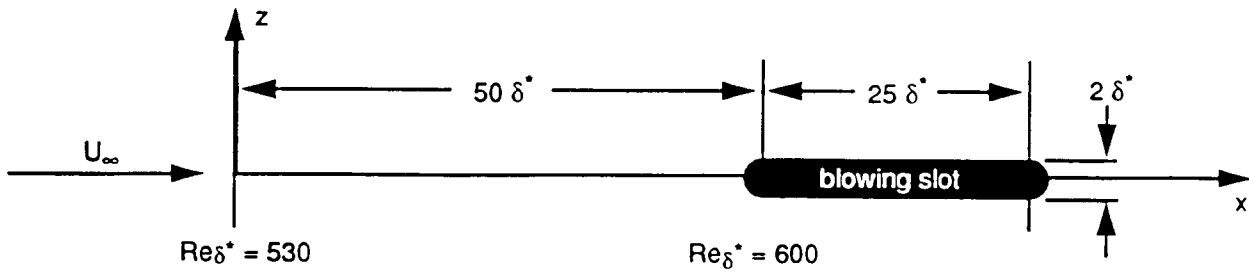
Figure 12: Plan view of high- ($p = 0.02$) and low-pressure ($p = -0.035$) regions at $t = 153.10$. The downstream edge of the vortex is at $x = 147.7$. The upstream end of the high-pressure region is at $x = 120.2$. The numbers indicate the order of appearance of the quasi-streamwise vortices.

Figure 13: Side view of low-pressure ($p = -0.035$) regions at $t = 153.10$. The Blasius profile is shown at the left at $x = 120.7$.

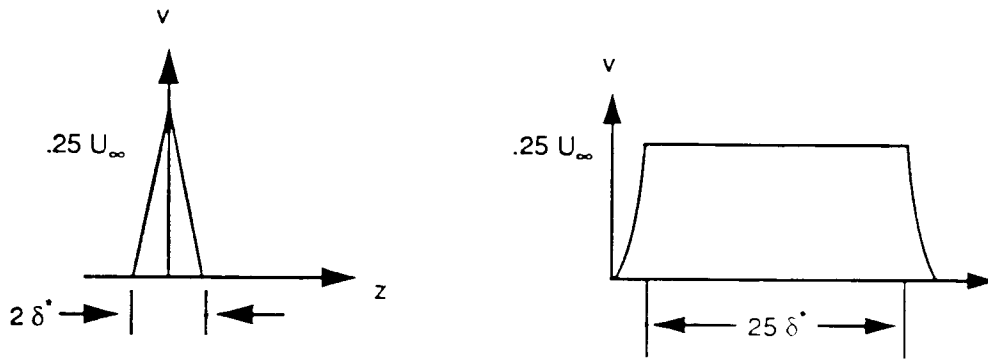
Figure 14: Plan view of the magnitude of perturbation streamwise velocity (bottom) and vertical vorticity (top) at $t = 150.10$, $y = 2.41$. The enveloping contours are $0.02U_0$ and $0.02U_0/\delta_0^*$ respectively. Contour increments are $0.05U_0$ for the velocity and $0.10U_0/\delta_0^*$ for the vorticity. The horizontal lines indicate the locations where $z = \pm 0.25$, i.e. the locations for the side views in the following figure.

Figure 15: Side view of the magnitude of perturbation streamwise velocity (bottom) and vertical vorticity (top) along $z = 0.25$ at $t = 150.10$. The enveloping contours are $0.02U_0$ and $0.02U_0/\delta_0^*$ respectively. Contour increments are $0.05U_0$ for the velocity and $0.10U_0/\delta_0^*$ for the vorticity. The horizontal lines on the bottoms indicate the wall locations. Velocity vectors appear at the left. The horizontal line extending beyond the velocity vectors indicates the position where $y = 2.41$, i.e. the location for the plan views in the previous figures.

Figure 16: Locally averaged ($120 \leq x \leq 132$, $|z| \leq 3.0$) profile in wall units at $t = 158.30$.



(a)



(b)



